

Evolution of time-symmetric gravitational waves: Initial data and apparent horizons*

Kenneth Eppley

University of Maryland, College Park, Maryland

(Received 4 March 1977)

Initial data were constructed numerically representing pure gravitational radiation with no sources or wormholes, under the conditions of time symmetry, axisymmetry, vacuum, and no rotation. The constraints were solved by making a conformal transformation on a base metric and solving the scale equation for the conformal factor. The initial data contain a black hole if the amplitude of the waves is sufficiently strong. The locations of apparent horizons were found for several such amplitudes. At a critical amplitude the throat pinches off and the geometry becomes singular.

The first attempt to construct spacetimes numerically was made about 15 years ago,¹ but we have only recently begun to obtain useful information from such studies. In problems such as the collision of two black holes² we have reached the point of being able to generate spacetimes containing radiation. We need methods to distinguish radiation from coordinate waves, and to calculate the energy carried by this radiation, or, rather, to find out which of the many methods that will work in principle are actually practical in a problem of this sort. An excellent test case to examine for this purpose is a spacetime which is pure radiation, such as the time-symmetric gravitational waves whose initial data were investigated by Brill some years ago.³ These are source-free waves of positive energy on a Euclidean topology, i.e., there are no wormholes. The condition of time symmetry is somewhat analogous to an electromagnetic wave at an instant of zero electric field, which could be produced by an imploding wave which comes in from infinity, reaches its point of greatest concentration (moment of time symmetry), and then disperses out again to infinity. While there exist electromagnetic waves which simply disperse, no one knows whether *any* gravitational wave, however weak it may be to start with, will remain forever nonsingular. It has been proved that a nonsingular evolution will exist for a finite time, but not for an indefinite time. So this is another question on which the study of the time-symmetric waves may shed light. Finally, for strong waves, one expects a collapse to a black hole. It should be interesting to compare what happens here to the cases of nonspherical collapse of matter fields currently being studied. This paper considers the numerical construction of initial data for such time-symmetric waves.

For this problem with the assumptions of axial symmetry, no rotation and time symmetry, we take as ansatz the following form of a base metric on an initial spacelike hypersurface:

$$\begin{aligned}
 ds^2 &= e^\alpha(d\rho^2 + dz^2) + \rho^2 d\phi^2, \\
 \text{i.e.,} \\
 \gamma_{\rho\rho} &= \gamma_{zz} = e^\alpha, \\
 \gamma_{\phi\phi} &= \rho^2, \\
 \gamma_{\rho z} &= \gamma_{\rho\phi} = \gamma_{z\phi} = 0 \\
 (\gamma_{ab} &\text{ is the three-dimensional metric.)}
 \end{aligned}
 \tag{1}$$

$\gamma_{\rho\phi}$ and $\gamma_{z\phi}$ are zero identically by nonrotation. Flat space corresponds to $q=0$. For time symmetry we have $K_{ab}=0$, so the momentum constraints automatically hold. We solve the Hamiltonian constraint by a conformal map:

$$\begin{aligned}
 \bar{\gamma}_{ab} &= \psi^4 \gamma_{ab}, \\
 \text{i.e.,} \\
 8D_a D^a \psi &= {}^3R\psi,
 \end{aligned}
 \tag{2}$$

where D_a is the covariant derivative and 3R is the Ricci scalar with respect to the base metric γ_{ab} . This is a linear elliptic equation which we solve numerically by relaxation methods.⁴

The quantity q is not entirely arbitrary but must satisfy the following restrictions:

$$\begin{aligned}
 q &= 0 \text{ when } \rho = 0 \text{ (} z \text{ axis) (by axial symmetry),} \\
 q_z &= 0 \text{ on } \rho \text{ axis,} \\
 \text{and} \\
 q &\sim 1/\gamma^2 \text{ or faster asymptotically.}
 \end{aligned}
 \tag{4}$$

Brill and Wheeler³ deduced a number of properties of solutions of (3), but were unable to find any choice of $q(x)$ for which they could solve (3) analytically. Thus they examined a nonphysical model—taking the scalar curvature to be a square well—which, they believed, should demonstrate qualitative behavior similar to actual solutions of (3).

They found that for the square-well potential the total mass is proportional to the square of the amplitude for small amplitudes, that the data contain a black hole for strong enough amplitudes, and

at a critical amplitude the throat pinches off. We will see below that these qualitative features are indeed found in numerical solutions of these equations. But a number of problems were left unsolved. No one had actually carried through this prescription for constructing initial data which could actually be part of a spacetime. The proportionality constant of m on A^2 was not known, nor was the value of the critical amplitude. Also, no one had attempted to determine the existence and location of apparent horizons for such initial data. All of these questions will be answered in this paper.

We used the following form as a trial function, because it is the simplest function which satisfied these restrictions with the least spatial variation:

$$q = \frac{A\rho^2}{1 + (r/\lambda)^n}, \quad (5)$$

where A, λ are constants, and $r^2 = \rho^2 + z^2$, and $n \geq 4$.

Brill³ has shown that the initial-value equation can be rewritten in the simple form:

$$\nabla^2 \psi = \Phi \psi, \quad (6)$$

where ∇^2 is the ordinary flat Laplacian in three-space and

$$\Phi \equiv \frac{1}{8}(q_{\rho\rho} + q_{zz}). \quad (7)$$

For our choice of q we obtain (taking $\lambda = 1$)

$$q_{\rho\rho} + q_{zz} = A[2U - n(4+n)\rho^2 U^2 r^{n-2} + 2n^2 \rho^2 r^{2n-2} U^3], \quad (8)$$

where

$$U \equiv (1 + r^n)^{-1}. \quad (9)$$

The boundary conditions on ψ are either that ψ goes to unity at spatial infinity or that ψ is unity at the origin. In the first case the asymptotic behavior for ψ will be

$$\psi = 1 + m/2r + O(1/r^2), \quad (10)$$

where m is the total mass of the configuration. To get the second normalization ψ is multiplied by an overall constant $c = \psi(0)^{-1}$, which changes the total mass by the factor c^2 .

There were a number of numerical problems to be solved to make ψ have the proper asymptotic behavior, and to be a consistent solution of the equation. The total mass of any configuration can be written in a number of different forms, which should give reasonable agreement if we are to believe our numerical construction. The basis expression is (with $\psi = 1$ at infinity)

$$m = -\frac{1}{2\pi} \int \vec{\nabla} \psi \cdot d\vec{s} \quad (G = c = 1), \quad (11)$$

which can be transformed to a volume integral

$$m = -\frac{1}{2\pi} \int \nabla^2 \psi d^3x \quad (\text{flat-space Laplacian}), \quad (12)$$

or, using (6),

$$m = -\frac{1}{2\pi} \int \Phi \psi d^3x. \quad (13)$$

Brill showed that this can be cast in a positive-definite form:

$$\begin{aligned} m &= -\frac{1}{2\pi} \int \vec{\nabla}(\ln \psi) \cdot d\vec{s} \\ &= -\frac{1}{2\pi} \int \left[\frac{\nabla^2 \psi}{\psi} - \left(\frac{\nabla \psi}{\psi} \right)^2 \right] d^3x \\ &= -\frac{1}{2\pi} \int \Phi d^3x + \frac{1}{2\pi} \int \left(\frac{\nabla \psi}{\psi} \right)^2 d^3x \\ &= \frac{1}{2\pi} \int \left(\frac{\nabla \psi}{\psi} \right)^2 d^3x, \end{aligned} \quad (14)$$

because, from (7), $\int \phi d^3x = 0$. One cannot expect exact agreement in a numerical solution. But in the first attempt to calculate the mass using a fairly fine mesh, we found the value from (11) two orders of magnitude larger than that from (14). Also disturbing was the fact that the surface integral was quite different from the volume integral, although they should be equal whether or not ψ satisfied the initial-value equations. This fact showed the importance of using a difference scheme which satisfied the conservative property. Such a scheme is one for which the difference operators are chosen to satisfy the macroscopic flux conservation theorems on a grid of finite size. The ordinary second-order accurate expression for the Laplacian in Cartesian or axial coordinates possesses this property, as we shall show.

Consider a unit volume produced by rotating a region $d\rho$ by dz located at ρ_c, z_c about the ϕ axis to make an annulus of volume $2\pi\rho_c \Delta\rho \Delta z$. Then Stokes's theorem through the sides of this volume gives

$$\begin{aligned} \int \nabla^2 \psi dV &\cong 2\pi\rho_c \Delta\rho \Delta z \nabla^2 \psi(\rho_c, z_c) \\ &= \psi_\rho \Delta z 2\pi\rho_c \Big|_{\rho_c + \Delta\rho/2} - \psi_\rho \Delta z 2\pi\rho_c \Big|_{\rho_c - \Delta\rho/2} \\ &\quad + \psi_z \Delta\rho 2\pi\rho_c \Big|_{z_c + \Delta z/2} - \psi_z \Delta\rho 2\pi\rho_c \Big|_{z_c - \Delta z/2} \end{aligned} \quad (15)$$

or

$$\begin{aligned} \nabla^2 \psi &\cong \frac{1}{\Delta\rho^2} [(1 + \Delta\rho/2\rho_c)\psi_{i,j+1} \\ &\quad - 2\psi_{i,j} + (1 - \Delta\rho/2\rho_c)\psi_{i,j-1}] \\ &\quad + \frac{1}{\Delta z^2} (\psi_{i+1,j} - 2\psi_{i,j} + \psi_{i-1,j}) \end{aligned} \quad (16)$$

(where we use j to denote the ρ direction and i for the z direction.) By construction the volume in-

tegral using this expression for $\nabla^2\psi$ will equal the surface integral over the boundary. Here the result agrees with the usual second-order formula:

$$\begin{aligned}\nabla^2\psi &= \psi_{\rho\rho} + \frac{1}{\rho}\psi_{\rho} + \psi_{zz} \\ &\cong \frac{1}{\Delta\rho^2}(\psi_{i,j+1} - 2\psi_{i,j} + \psi_{i,j-1}) \\ &\quad + \frac{1}{2\rho\Delta\rho}(\psi_{i,j+1} - \psi_{i,j-1}) \\ &\quad + \frac{1}{\Delta z^2}(\psi_{i+1,j} - 2\psi_{i,j} + \psi_{i-1,j}).\end{aligned}\quad (17)$$

However, on a nonuniform or stretched mesh, or in nonflat coordinates, the ordinary operator will not in general be conservative. For example, we used a quadratic scaling of the grid:

$$z = \eta + c\eta^2, \quad (18)$$

$$\rho = \xi + c\xi^2,$$

so

$$\psi_x = s\psi_\eta, \quad (19)$$

$$\psi_{xx} = s^2\psi_{\eta\eta} - 2cs^3\psi_\eta \quad [s \equiv \eta_x = (1 + 2c\eta)^{-1}].$$

Consider just the ψ_{xx} term in the Laplacian:

$$\begin{aligned}\psi_{xx}\Delta z &= \frac{\Delta\eta}{s_i} \left[\frac{s_i^2}{\Delta\eta^2}(\psi_{i+1} - 2\psi_i + \psi_{i-1}) \right. \\ &\quad \left. - \frac{c}{\Delta\eta} s_i^3(\psi_{i+1} - \psi_{i-1}) \right].\end{aligned}\quad (20)$$

This is not the same as $\psi_x|_{x+\Delta x/2} - \psi_x|_{x-\Delta x/2}$, which equals

$$\begin{aligned}\frac{1}{2\Delta\eta} [s_{i+1/2}(\psi_{i+1} - \psi_i) - s_{i-1/2}(\psi_i - \psi_{i-1})] \\ \cong \frac{1}{4\Delta\eta} [(s_{i+1} + s_i)(\psi_{i+1} - \psi_i) - (s_{i-1} + s_i)(\psi_i - \psi_{i-1})].\end{aligned}\quad (21)$$

If we had used (21) to obtain the difference operator for ψ_{xx} , then its volume integral would have equaled the surface integral, but if we had used (20) it would not have. If we need to solve an initial-value problem in general nonflat coordinates, we can use the above algorithm to construct a covariant differential Laplacian which will be conservative.

The error introduced by the nonconservative form (20) was not trivial, even on quite fine grids, and could amount to almost an order-of-magnitude difference between the masses given by (11) and (12). However, even using a uniform grid on which these integrals agreed, they still differed from (14) by over another order of magnitude. It was necessary to go to a fourth-order accurate scheme to get all the masses to agree. There is no unique way of writing a fourth-order differencing operator, so

we used the common Taylor series method for obtaining difference expressions. Then we express the first derivatives on the right-hand side of (15) at the point $i + \frac{1}{2}$ (for example) by

$$\psi_x|_{i+1/2} \cong \frac{9}{8\Delta z}(\psi_{i+1} - \psi_i) + \frac{1}{24\Delta z}(\psi_{i-1} - \psi_{i+2}). \quad (22)$$

Thus we get a fourth-order conservative expression for the Laplacian in axial coordinates:

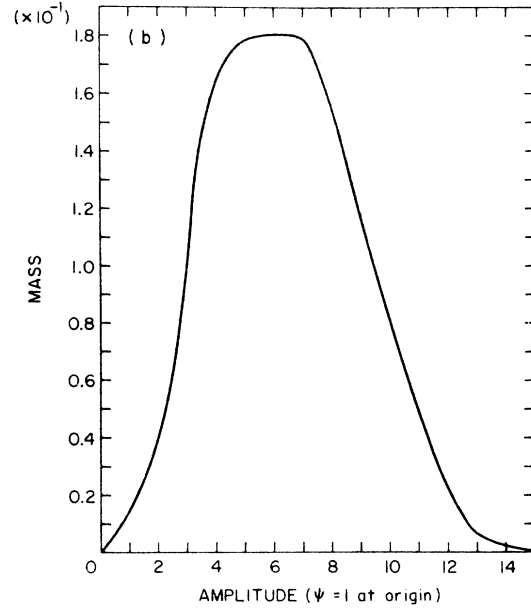
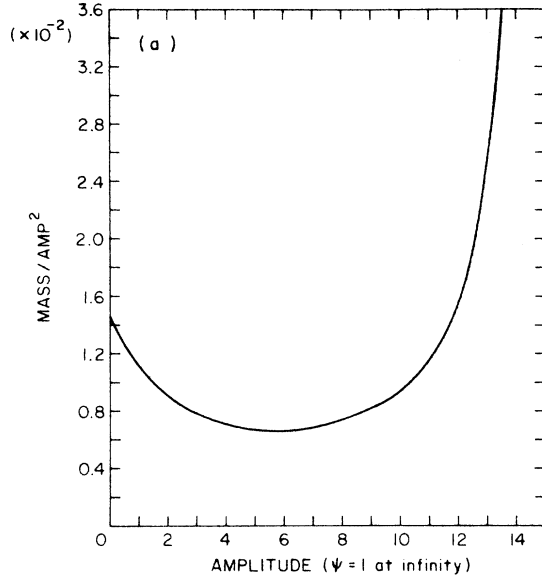


FIG. 1. Variation of mass with amplitude for two normalizations of ψ . ($\lambda=1$, $n=5$, using a 50×50 mesh with a step size of 0.2). (a) $\psi=1$ at infinity. We plot m/A^2 versus A . m/A^2 goes to infinity at the pinch-off point. (b) $\psi=1$ at the origin. We plot m versus A . The mass goes to zero at the pinch-off.

$$\begin{aligned} \nabla^2 \psi = & \frac{1}{96\Delta\rho^2} [(-1-d)\psi_{i,j+2} + (d-1)\psi_{i,j-2} + (28+26d)\psi_{i,j+1} + (28-26d)\psi_{i,j-1} - 54\psi_{i,j}] \\ & + \frac{1}{96\Delta z^2} [-\psi_{i+2,j} - \psi_{i-2,j} + 28(\psi_{i+1,j} + \psi_{i-1,j}) - 54\psi_{i,j}], \end{aligned} \quad (23)$$

where $d \equiv \Delta\rho/2\rho_c$.

Using this operator to solve for ψ [by the usual successive overrelaxation (SOR) method] the mass integral (11) agreed with (14) to about 30% on a 50×50 uniform grid (with step size 0.2). It is worth noting that the positive-definite expression was by far the most invariant under all changes of grid size, differencing scheme, etc., giving essentially the same mass for the second-order scheme on the stretched grid as for the fourth-order scheme on the uniform grid. Thus it would be worth trying to cast the mass into a positive-definite form for other spacetimes when at all possible. We plot the mass as a function of A in Fig. 1.

A further advantage of the fourth-order scheme was evident at strong amplitudes near the pinch-off point. The second-order method required superfine grids near the origin to get any solution, and could not reliably distinguish the amplitudes above the pinch-off from those below. With the fourth-order scheme only a moderately fine grid (step size 0.1 with $\lambda = 1$) was adequate for all amplitudes, and it was clear where the pinch-off occurred, as the relaxation converged below the critical amplitude and diverged above it. We will discuss the behavior of these strong amplitudes further in the next section.

Locating apparent horizons

As we increase the amplitude (holding λ fixed) the "cloud" of radiation becomes more and more concentrated. When it becomes sufficiently strong a black hole will form. This event is signaled by the sudden appearance of an apparent horizon, i.e., a marginally trapped surface.⁵ On a time-symmetric surface this is equivalent to the existence of a surface of minimal area, or "throat." The formation of a throat can be visualized by constructing embedding diagrams of the geometry. While it is a difficult task to embed the entire surface, it is simple to embed the equatorial plane, due to its rotational symmetry. One can write the embedding explicitly by demanding that the metric on the equator equal that of a surface of rotation $z(x, y)$ in Euclidean space.⁶ We set

$$\begin{aligned} x &= F(\rho) \cos\varphi, \\ y &= F(\rho) \sin\varphi, \\ z &= G(\rho), \end{aligned} \quad (24)$$

then

$$\begin{aligned} ds^2 &= dx^2 + dy^2 + dz^2 \\ &= (F_\rho^2 + G_\rho^2) d\rho^2 + F^2 d\varphi^2 \\ &= \gamma_{\rho\rho} d\rho^2 + \gamma_{\varphi\varphi} d\varphi^2 \quad (\text{on the equator}) \\ &= \psi^4 (e^a d\rho^2 + \rho^2 d\varphi^2); \end{aligned} \quad (25)$$

thus

$$\begin{aligned} F &= \rho\psi^2, \\ F_\rho &= \psi^2 + 2\rho\psi\psi_\rho, \\ G &= \int d\rho (\psi^4 e^a - F_\rho^2)^{1/2} \end{aligned} \quad (26)$$

defines a surface $z(x, y)$ on the equator whose intrinsic geometry is that of the time-symmetric wave. We show such embeddings in Fig. 2. Note the appearance of the throat when the amplitude is increased.

While these embeddings tell us the approximate amplitude for which a black hole exists, to determine the exact amplitude and to find the shape of the apparent horizon we need to solve the trapped surface equation⁵

$$(\gamma^{ab} - s^a s^b)(D_a s_b - K_{ab}) = 0, \quad (27)$$

where s^a is the spacelike normal to the two-surface which is the horizon. We can rewrite this (the following is due to Eardley⁷)

$$s_B (u^A D_A) u^B = -\mathcal{H} - \gamma^{\varphi\varphi} \Gamma_{\varphi\varphi}^A s_A, \quad (28)$$

where

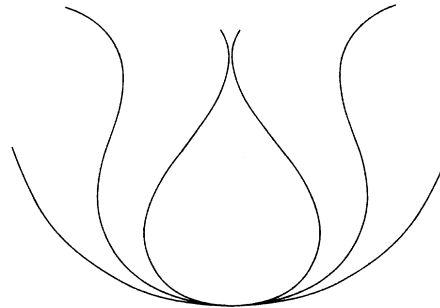


FIG. 2. Embedding of the equatorial geometry into Euclidean space. The three embeddings are for amplitudes $A = 2, 5,$ and $15,$ respectively.

$$\mathfrak{H} \equiv (\gamma^{ab} - s^a s^b) K_{ab} = u^A u^B D_A s_B - \gamma^{\varphi\psi} \Gamma_{\varphi\psi}^A s_A,$$

and u^A is the tangent vector to the horizon. Then

$$s_B \frac{D^2 x^B}{ds^2} = -\mathfrak{H} - \gamma^{\varphi\psi} \Gamma_{\varphi\psi}^A s_A, \quad (29)$$

where s is the arc length along the curve. If $s = s(\lambda)$ then

$$s_B \left(\frac{ds}{d\lambda} \right)^{-2} \left[\frac{D^2 x^B}{d\lambda^2} - \left(\frac{ds}{d\lambda} \right)^{-1} \frac{d^2 s}{d\lambda^2} \frac{dx^B}{d\lambda} \right] = -\mathfrak{H} - \gamma^{\varphi\psi} \Gamma_{\varphi\psi}^A s_A$$

or

$$s_B \frac{D^2 x^B}{d\lambda^2} = - \left(\frac{ds}{d\lambda} \right)^2 \gamma^{\varphi\psi} \Gamma_{\varphi\psi}^A s_A - \left(\frac{ds}{d\lambda} \right)^2 \mathfrak{H}, \quad (31)$$

since

$$s_B \left(\frac{ds}{d\lambda} \right)^{-1} \frac{dx^B}{d\lambda} = s_B \frac{dx^B}{ds} = s_B u^B = 0.$$

Defining (A, B, C) go over coordinates $(1, 2)$

$$m_B \equiv \frac{1}{(2\gamma)^{1/2}} \frac{ds}{d\lambda} s_B = \epsilon_{BC} \frac{dx^C}{d\lambda} = \left(\frac{dx^{(2)}}{d\lambda}, -\frac{dx^{(1)}}{d\lambda} \right), \quad (32)$$

then

$$m_B \frac{D^2 x^B}{d\lambda^2} = - \left(\frac{ds}{d\lambda} \right)^2 \gamma^{\varphi\psi} \Gamma_{\varphi\psi}^A m_A - \frac{1}{(2\gamma)^{1/2}} \left(\frac{ds}{d\lambda} \right)^3 \mathfrak{H}. \quad (33)$$

Now using $\lambda = \theta, x^{(1)} = r, x^{(2)} = \theta, x^{(3)} = \phi$, (33) becomes the following:

$$\begin{aligned} r_{\theta\theta} &= -\Gamma_{BC}^A m_A \frac{dx^B}{d\theta} \frac{dx^C}{d\theta} \\ &\quad - \left(\frac{ds}{d\theta} \right)^2 \gamma^{\varphi\psi} \Gamma_{\varphi\psi}^A m_A - \frac{1}{(2\gamma)^{1/2}} \left(\frac{ds}{d\theta} \right)^3 \mathfrak{H}. \end{aligned} \quad (34)$$

Now using

$$\left(\frac{ds}{d\lambda} \right)^2 = \gamma_{AB} \frac{dx^A}{d\theta} \frac{dx^B}{d\theta}, \quad (35)$$

$$\mathfrak{H} = \left(\frac{ds}{d\theta} \right)^{-2} \frac{dx^A}{d\theta} \frac{dx^B}{d\theta} K_{AB} + \gamma^{\varphi\psi} K_{\varphi\psi},$$

then

$$\begin{aligned} r_{\theta\theta} &= -\Gamma_{BC}^A m_A \frac{dx^B}{d\theta} \frac{dx^C}{d\theta} - \gamma_{BC} \frac{dx^B}{d\theta} \frac{dx^C}{d\theta} \Gamma_{\varphi\psi}^A m_A \gamma^{\varphi\psi} \\ &\quad - \frac{1}{(2\gamma)^{1/2}} \left(\gamma_{AB} \frac{dx^A}{d\theta} \frac{dx^B}{d\theta} \right)^{1/2} \frac{dx^C}{d\theta} \frac{dx^D}{d\theta} K_{CD} \\ &\quad - \frac{1}{(2\gamma)^{1/2}} \left(\gamma_{AB} \frac{dx^A}{d\theta} \frac{dx^B}{d\theta} \right)^{3/2} \gamma^{\varphi\psi} K_{\varphi\psi}, \end{aligned}$$

where

$$\begin{aligned} x^A &= (r, \theta), \\ m^A &= (1, -r_\theta), \\ \frac{dx^A}{d\theta} &= (r_\theta, 1). \end{aligned} \quad (36)$$

Using $K_{aB} = 0$ and (1) this simplifies to

$$\begin{aligned} r_{\theta\theta} + \frac{r_\theta^3}{r^2} \left(q_\theta/2 + \frac{4\psi_\theta}{\psi} + \cot\theta \right) + r_\theta^2 \left[-\frac{3}{r} - \left(\frac{q_r}{2} + \frac{4\psi_r}{\psi} \right) \right] \\ + r_\theta \left(q_\theta/2 + \cot\theta + \frac{4\psi_\theta}{\psi} \right) - \left[2r + r^2 \left(q_r/2 + \frac{4\psi_r}{\psi} \right) \right] = 0. \end{aligned} \quad (37)$$

However, the method we devised to solve this equation should work equally well with the general case (36). We solve this equation to find the surface $r(\theta)$. The method that worked best was to write r as a power series in $\cos(\theta)$ (much as Brill and Lindquist did in constructing minimal surfaces⁸).

$$r(\theta) = \sum_{n=0}^{n_{\max}} c_n \cos^n \theta. \quad (38)$$

Then (38) becomes

$$P(c_0, c_1, \dots, c_n, \dots, \theta) = 0 \text{ for all } \theta. \quad (39)$$

Starting with an initial guess, each c_n was varied to find the minimum of $\int P d\theta$ with the other coefficients fixed. The procedure was iterated to find the minimum over all the c_n . When the amplitude was too weak, the solution converged to a point at the origin. For amplitudes $A \geq 5$ (with $n=5, \lambda=1$) the solution converged to a nonzero curve very close to the throat located by the embeddings. As the amplitude increases, the horizon moves further out and becomes more spherical, until it pinches off at $A \cong 16$. The horizons are shown in Fig. 3, using the normalization $\psi=1$ at the origin (making it easier to present all the results on the same scale). The occurrence of the horizon and the pinch-off does not depend on the normalization, but the embeddings will of course appear different. With $\psi=1$ at infinity, the mass goes to infinity rather than to zero at pinch-off. The

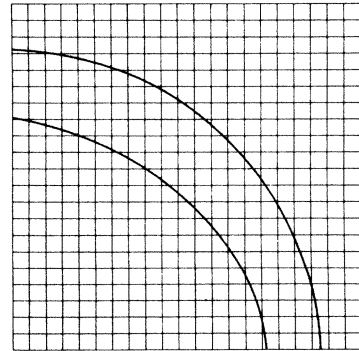


FIG. 3. Location of apparent horizons. The inner curve is for $A=5$, where the horizon first appears. The outer curve is for $A=15$, just before the pinch-off (shown for $\lambda=1, n=5$, step size of 0.05).

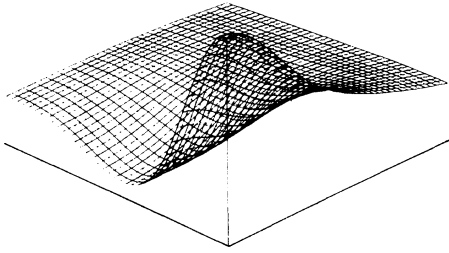


FIG. 4. Plot of conformal factor ψ which solves initial-value equations for $A=15$, $\lambda=1$, $n=5$, step size 0.05. The vertical axis gives the magnitude of ψ , on a scale from zero to 1. The axis to the right is the symmetry axis (z axis) and the axis to the left is the equator (ρ axis).

embeddings become more stretched out at the base as they pinch in at the throat. The conformal factor itself near pinch-off is shown in Fig. 4.

In future papers we will describe how we evolved

these initial data, both for weak "clouds" of radiation which disperse to infinity, and for strong waves which collapse to a black hole. We will describe several ways to calculate the energy flux carried by this radiation, and show the spatial and temporal distribution of the radiation pattern.

ACKNOWLEDGMENTS

I gratefully acknowledge the help of John Wheeler, who suggested this investigation. Larry Smarr and Douglas Eardley contributed very heavily to much of this work. I am also indebted to James York and Paul Sommers for their encouragement and suggestions, as well as to Dieter Brill, Charles Misner, Robert Gowdy, and the rest of the relativity group at the University of Maryland, and to James Wilson, James LeBlanc, and many others at the Lawrence Livermore Laboratory.

*Research partially supported by NSF under Grants Nos. NPS74-14191-A01 to Univ. of North Carolina and PHY70-02077A04 to Univ. of Maryland.

¹S. G. Hahn and R. W. Lindquist, *Ann. Phys. (N.Y.)* **29**, 304 (1964).

²L. Smarr, A. Cadez, B. DeWitt, and K. Eppley, *Phys. Rev. D* **14**, 2443 (1976); L. Smarr, in *Eighth Texas Symposium on Relativistic Astrophysics*, 1977 (unpublished).

³D. Brill, Ph.D. thesis, Princeton University, 1959 (unpublished); *Ann. Phys. (N.Y.)* **7**, 466 (1959); J. A. Wheeler,

in *Relativity, Groups and Topology*, edited by C. De Witt and B. DeWitt (Gordon and Breach, New York, 1964).

⁴K. Eppley, Ph.D. thesis, Princeton University, 1975 (unpublished).

⁵S. W. Hawking and G. F. R. Ellis, *The Large Scale Structure of Spacetime* (Cambridge Univ. Press, London, England, 1973).

⁶L. Smarr, *Phys. Rev. D* **7**, 2814 (1973).

⁷D. Eardley, 1976 (private communication).

⁸D. Brill and R. W. Lindquist, *Phys. Rev.* **131**, 471 (1963).